



Linear Quadratic Integral optimal control of photovoltaic systems

Mostafa Rahideh ^{1,*}, Abolfazl Halvaei Niasar ¹, Abbas Ketabi ¹, Iman zamani ²

¹ Faculty of Electrical and Computer Engineering, University of Kashan, Kashan, Iran

² Electrical and Electronic Engineering Department, Shahed University, Tehran, Iran

ABSTRACT: This study aims to report on the application of Linear Quadratic Integral (LQI) based global maximum power point tracker (GMPP) method for transferring the available maximum power from photovoltaic (PV) systems to load in unshaded and shaded conditions. For the maximum power transmission under varying the environmental conditions and partially shaded conditions, MPPT technologies are utilized in PV systems. For the improvement of functioning MPPT, a new two-level control structure which decreases difficulty in the control process and efficiently deals with the uncertainties in the PV systems is introduced. In the proposed approach, the reference voltage at the global maximum power point (GMPP) is estimated by a new scanning algorithm. The difference between the reference voltage and the voltage of the PV array is then used by LQI controller to generate the duty cycle for a boost converter. The design process of the proposed approach is explained as step by step. The benefits of the approach are quicker tracking capability, transferring maximum deliverable power and simple implementation. To verify the proposed method, several irradiation profiles that create several peaks in the P-V curve are used. The simulation results show that the proposed method causes PV systems to track the GMPP immediately so that no oscillation around the GMPP is observed. Therefore, maximum efficiency can be derived from the PV system.

Review History:

Received: 2019-05-04

Revised: 2019-10-30

Accepted: 2019-10-30

Available Online: 2020-12-01

Keywords:

Photovoltaic systems

Maximum power point tracking (MPPT)

Linear Quadratic Integral optimal control

1. INTRODUCTION

The reduction of fossil fuels and growth in energy demand have led to an interest in using renewable energy resources. Environmental issues arise because of conventional power generation. The renewable energy source because of its clean, green, and readily available nature has become essential to utilize it for the generation of reliable energy and, at the same time, meet energy demand. Photovoltaic (PV) system draws its attention as it happens to be one of the promising energy resources. It is preferred for the following reasons: zero fuel cost, no pollution, reduced maintenance, and noise free nature. Though there are advantages, it introduces two main factors that affect the implementation of the photovoltaic system. The factors are high installation cost and low conversion efficiency. A viable solution to increase efficiency is to introduce Maximum Power Point Tracking, commonly referred to as MPPT. MPPT is achieved by adopting various tracking methods.

The process of extracting maximum available power from a power source such as a PV module whose output changes more often based on the environmental conditions is MPPT. The generated power in the module is a function of both solar irradiation and temperature. Hence, when there is a change in the solar irradiation or temperature or both, the module power varies. In such situations, the fixed load connected

*Corresponding author's email: mostafarahideh97@gmail.com

across the PV unit will experience a change in its impedance. It becomes impossible to derive the maximum power unless the source and load impedances are matched [40]. Changing the load impedance to match the source impedance forms the basis of MPPT. The MPP tracking is achieved by placing a power converter between source and load which matches the impedance of the module with the impedance at the input of the converter that makes maximum power transfer possible. Either a dc-dc converter or an ac-dc converter is used depending on the load to serve the purpose. Not only the converter changes the power from one form to another, but it also ensures transferring maximum power at any instant [41].

Several methods are reported in the literature for MPPT. Each method has advantages and limitations over the other methods and varies in terms of complexity, sensor requirement, tracking speed, and cost [22-38].

The most widely used MPPT methods can be divided into two groups: hill climbing methods such as Perturb and Observer (P&O) and Incremental Conductance (INC), and constant voltage methods [1-4]. Starting from the standard implementations, other technical solutions [5-18] have been proposed in order to improve the accuracy and dynamic behavior of the tracking controls. On the other hand, most of them neglect that MPPT is a multimodal optimization problem [19] since there are local optima in the P-V characteristic curve when not uniform irradiance occurs over



the photovoltaic system.

Considerable research efforts have been directed toward the development of more sophisticated MPPT algorithms able to identify the Global Maximum Power Point (GMPP) in order to extract the whole available power from the PV system under partially shaded conditions [20–33]. The computational burden, range of effectiveness and convergent speed of these algorithms is quite different and depends on the adopted theoretical methodology. Some methods determine the GMPP by exploiting deterministic searching algorithms such as constant power operation [21], dividing rectangles (DIRECT) method [22], restricted voltage window search algorithm [25], Cuckoo search [30], while other MPPT algorithms are based on metaheuristic approaches such as the particle swarm optimization [20] and Artificial Neural Networks (ANNs) [26]. More in general, in the field of multimodal optimization the Evolutionary Algorithms [34], e.g. genetic algorithms [35], applying niching strategies [36] are designed to properly address multimodal functions. Furthermore, some niching algorithms are coupled with Deterministic Methods (DMs) [37] to enhance the final solution accuracy [38]. The basic idea is to firstly search the global optimum using a niching algorithm and, then the DM starts from the provided solution to draw up to the actual optimum. Therefore, a further distinction among algorithms that can be adopted to MPPT concerns the number of stages that the MPPT algorithms use. In fact, some techniques track the GMPP by using a unique procedure, while other methods identify the GMPP by adopting two stages. The latter ones, firstly adopt an algorithm to identify the “hill” where the GMPP is potentially located, and then a further algorithm is employed to reach the GMPP. In this perspective, the use of metaheuristic approaches coupled with a DM seems a good solution provided that information about the solar irradiance distribution on the panels and/or their temperature as well as the knowledge of the system model are given. Actually, these techniques could be applied without the use of a model, but the approach becomes very harmful because each objective function evaluation calls for changing the PV voltage in order to measure the current.

Hence, the methods mentioned until now need the measurement of solar irradiation over the panel and their temperature, and/or the scansion of a large portion of the PV characteristic to suitably determine the GMPP. Accordingly, the main limitation of the first kind of techniques is the necessity of using additional sensors and properly system models, whereas the main limitation of the second ones is the loss of energy due to the time spent to sample the PV characteristic. In this perspective, in [39] a technique based on the DIRECT search algorithm (first stage) and a suitable P&O algorithm (second stage) has been proposed. More in general, the aforementioned techniques have been designed for PV system placed in fixed installation, where the shading phenomena does not suddenly and frequently change as in case of installations on the roof of electric vehicles. In this case, a very accurate and fast GMPP tracking is necessary in order to maximize the extracted energy, taking into account

that the PV system operates under the high probability that the solar irradiance on the panel is not uniformly distributed, especially due to the presence of other vehicles, buildings and any other obstacles that blocks or refracts the solar rays impacting the PV modules, and this distribution continuously changes meanwhile the vehicle moves in the traffic.

In order to overcome the aforementioned limitations, the paper aims to study the effectiveness of an LQI based GMPPT approach whose goal is to quickly and accurately estimate the GMPP when no information about the solar irradiance distribution over the modules and their temperature is given, and when the PV system is subjected to continuously and rapidly changing shadowing patterns. Few measures are used to estimate the GMPP by means of the proposed GMPPT, and they are set a priori. Consequently, the estimation time is small and fixed. A new scanning algorithm is proposed to estimate the reference voltage at the GMPP. The estimated voltage is used by the LQI controller to generate the duty cycle for a boost converter.

The main contribution in this research work is the design and validation of a new scanning algorithm of reference PV voltage and a Linear Quadratic Integral optimal control (LQI) for a standalone PV system consisting of a boost converter that can track GMPP in the all environmental situations. The results obtained for the proposed GMPPT are compared with the conventional P&O method another new method. Since P&O method is the simplest and widely used accepted method, it is chosen for comparison.

2. MODEL DESCRIPTION

2.1. PV array model

The solar cell is a p-n semiconductor that has similar characteristics to diodes. Fig. 1 draws the equivalent circuit of a solar cell. The current source generates the photocurrent I_{ph} , which is relative to the irradiation. The following equation describes the relationship between the array terminal current and the voltage [43]:

$$V_{PV} = \frac{nKT}{q} \ln \left(\frac{I_{sc}}{I_{PV}} + 1 \right) \tag{1}$$

$$I_{PV} = I_L - I_{PVO} \left[\exp \left(\frac{q(V_{PV} + I_{PV}R_s)}{nKT} \right) \right] - \frac{V_{PV} + R_s I_{PV}}{R_{sh}} \tag{2}$$

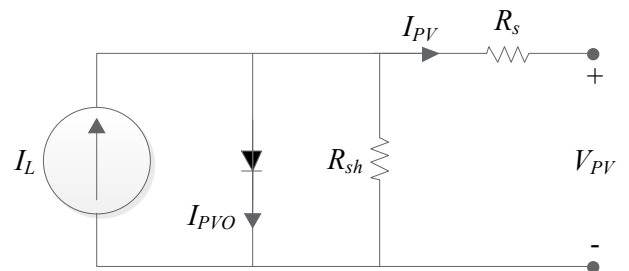


Fig. 1. Equivalent circuit of a solar cell

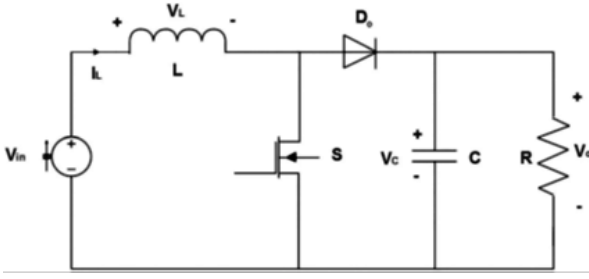


Fig. 2. General configuration of the boost converter

where

R_s : the series resistance

R_{sh} : the shunt resistance

I_L : the photo current

n : the diode ideality factor

R_s : is the diode saturation current

V_T : the thermal voltage

K : Boltzmann constant

q : is the electronic charge

The I_{sc} is a function of incident solar radiation G (W/m^2) and temperature and it is given by:

$$I_L = I_{L(T_1)} (1 + K_O (T - T_1)) \quad (3)$$

$$I_{L(T_1)} = G I_{sc(T_1, nom)} / G_{(nom)} \quad (4)$$

$$K_O = (I_{sc(T_2)} - I_{sc(T_1)}) / (T_2 - T_1) \quad (5)$$

where:

$G(nom)$: rated irradiation

T_1 : first temperature ($25^\circ C$)

T_2 : second temperature ($75^\circ C$)

T : ambient temperature

$I_{sc(T_1)}$: the rated short circuit current under rated irradiation ($1Sun=1000 W / m^2$) and in temperature T_1

$I_{sc(T_2)}$: the short circuit current in temperature T_2 . and the reverse saturation current is given by:

$$I_O = I_{O(T_1)} (T / T_1)^{3/n} e^{-qE_g/nk(1/T-1/T_1)} \quad (6)$$

$$I_{O(T_1)} = (I_{sc(T_1)} / e^{qV_{OC(T_1)}/nkT_1} - 1) \quad (7)$$

E_g : based gap voltage.

$V_{OC(T_1)}$: open circuit voltage per cell at temperature T_1 .

2.2.Small signal modeling of boost converter

When a dc-dc converter matches the source and load, the maximum power transfers from source to load. In this paper, a boost converter is selected to increase the module voltage to the level required by the load. Fig. 2 shows the general configuration of a boost converter. In the view of power

conservation, the source current is always more than the load current [44]. The converter can be modeled by a source, capacitor, inductor, switch, and a load. To boost up the output voltage, the inductor is placed at the front of the switching network. Following are the assumptions made for the boost converter [44]:

I. All components are lossless and ideal.

II. The time period is T of which switch is closed and opened for periods DT and $(1-D)T$, respectively, and operates in Continuous Conduction Mode.

III. The capacitor is selected such that output voltage is a constant one.

It becomes essential to model the converter to design a control system. In particular, modeling is required to understand how variations in the parameters such as input voltage, duty cycle, and load current have affected the output voltage. But knowing the dynamic behavior has become tedious because of the nonlinear time-varying nature of the switching process. This problem can be overcome by the use of small signal modeling. The state variables chosen are output voltage V_o and inductor current I_L , and the expressions during turn on and turn off processes are written as:

When the switch is ON:

$$L \frac{dI_L}{dt} = V_{in} \quad (8)$$

$$C \frac{dV_o}{dt} = -\frac{V_o}{R_L} \quad (9)$$

When the switch is OFF:

$$L \frac{dI_L}{dt} = V_{in} - V_o \quad (10)$$

$$C \frac{dV_o}{dt} = I_L - \frac{V_o}{R_L} \quad (11)$$

Introducing perturbation in state variables and equating ac and dc quantities neglecting second order terms, we get

$$L \frac{dI_L}{dt} = V_{in} - (1-D)V_o - V_o d \quad (12)$$

$$C \frac{dV_o}{dt} = (1-D)I_L - \frac{V_o}{R_L} - I_L d \quad (13)$$

Taking Laplace transform for equations (12) and (13) and arranging the control to input transfer function become

$$\frac{I_L(s)}{d(s)} = \frac{R_L C V_o s + 2(1-D)I_L R_L}{R_L L C s^2 + L s + R_L (1-D)^2} \quad (14)$$

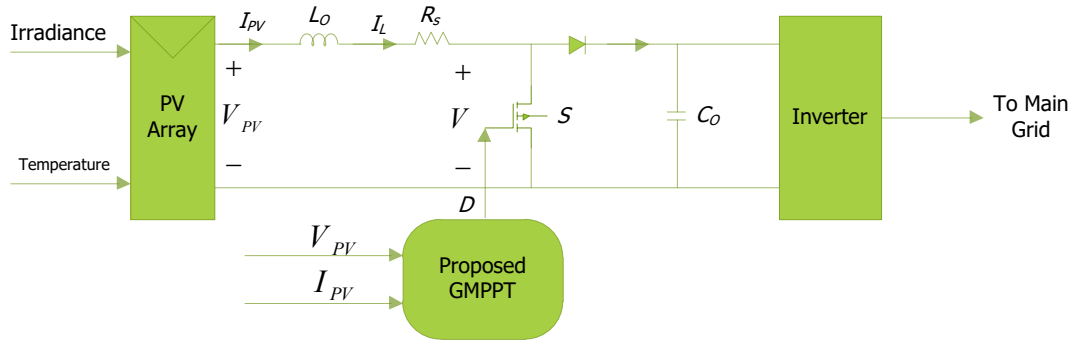


Fig. 3. PV-system under study

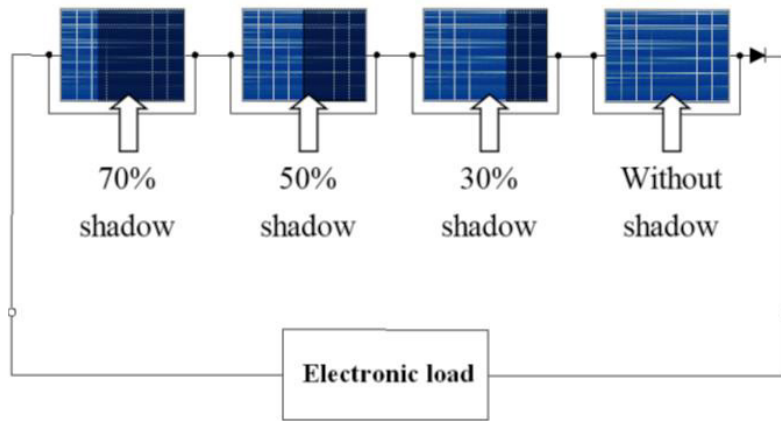


Fig. 4. A PV array consisting of unshaded and shaded modules

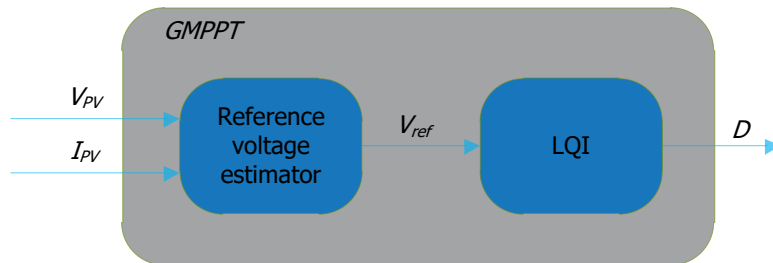


Fig. 5. The structure of the proposed GMPPT

In the above equation, V_o is the output voltage, L is the inductance, C is the capacitance, and D is the nominal duty cycle. The boost converter component values are indicated in Appendix 1.

3. SYSTEM UNDER STUDY

The complete block diagram of a photovoltaic system with proposed approach based GMPPT is shown in Fig. 3. The system consists of PV module, power converter, the proposed approach to track GMPP and a three-phase grid. The proposed approach ensures the extraction of maximum power from the PV module at any environmental conditions (normal and partial shading conditions). The proposed approach is designed to generate duty cycle D which when effected on the controller can effectively allow the panel impedance to match

with source impedance thereby extracting maximum power.

4. EFFECT OF PARTIAL SHADING CONDITION ON A PV

If there is not a shadow condition, an M -series N -parallel module array generates an output voltage $M \times V_{mpp}$ (where the V_{mpp} is PV voltage at maximum power point), an output current $N \times I_{mpp}$ (where the I_{mpp} is PV current at maximum power point) and an output power $M \times N \times P_{mpp}$ (where the P_{mpp} is PV power at maximum power point) at the MPP. According to Fig. 4, if there are variously shaded PV modules in a PV array, the output power is no longer equal to the unshaded case. The variously shaded case causes a multiple peak value problem and disables a maximum power point tracker for finding the MPP.

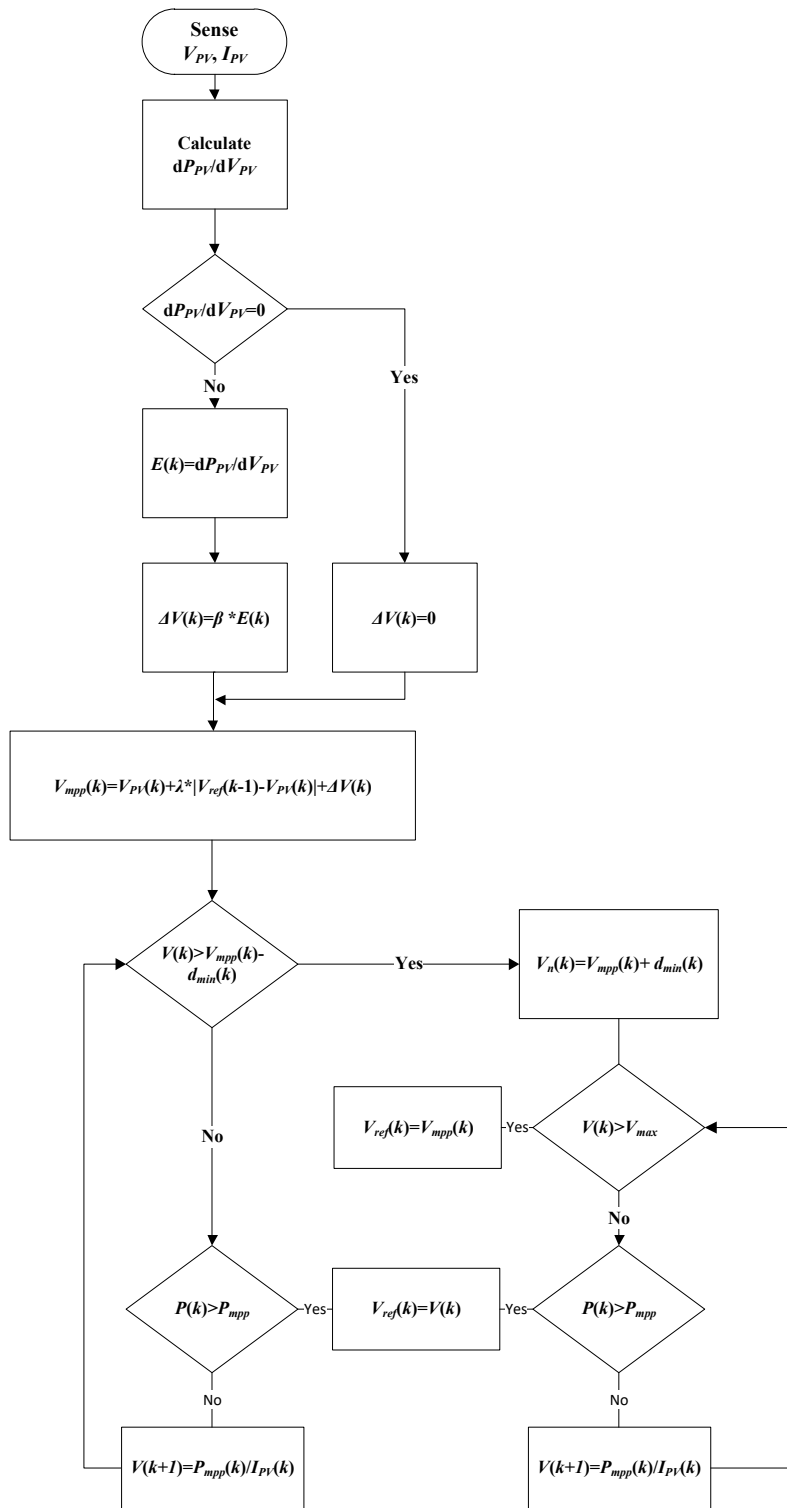


Fig. 6. The flowchart of the reference voltage estimation

5. PROPOSED METHOD

Fig. 5 illustrates the block diagram of the proposed GMPPT. In this study, a two-level control algorithm is suggested to perform the GMPPT tasks. It is clear from Fig. 5 that the suggested GMPPT has a reference voltage estimation block, an LQI block. The output of GMPPT is generated based on the reference voltage block and then applied to the boost converter. The duty cycle D is computed by the LQI using the

estimated reference voltage.

In the next subsections, the design method of the proposed approach is explained as step by step.

5.3. Reference voltage estimator block

Fig. 6 displays the suggested algorithm to estimate V_{ref} . This approach monitors and checks the operating voltage and current of the PV module at any moment. The slope sign is

determined in the power curve. The calculated slope is then used for generating the voltage at the maximum power point. If the sign of slope is positive, then V_{mpp} is enhanced and vice versa. The constant parameters β and λ are used to keep under control the closing speed to V_{mpp} . After determining V_{mpp} , the algorithm begins to check a number of points on the P-V curve in the range of V_{min} and V_{max} , where V_{min} and V_{max} are the minimum possible voltage for the PV array and the open circuit voltage of the PV array. Also, the minimum distance between local MPPs is obtained by

$$d_{min} = \frac{V_{mppoc}}{n_{bd}} \tag{15}$$

where V_{mppoc} is the voltage of MPP nearest to the open-circuit voltage V_{oc} and n_{bd} indicates the number of bypass diodes. The search begins from V_{min} and the relevant power is saved. If the saved power is greater than the primarily located MPP, then the current position is considered as the operating point and the reference voltage is obtained. If the saved power is less than the primarily located MPP then a new voltage sample is determined by

$$V(n+1) = \frac{V_{mpp}(n)I_{mpp}(n)}{I_{PV}(n)} = \frac{kI_{sc}(n)V_{mpp}(n)}{I_{PV}(n)} \tag{16}$$

where k is always a constant less than 1. The searching mechanism repeats the abovementioned steps and compares the new saved power with the primarily located MPP. This repeats until the whole P-V curve is scanned and or a greater power is found.

5.4.LQI block

As stated before, the LQI block accepts the reference voltage generated by the reference voltage estimator and generates the duty cycle which is applied to the DC-DC boost converter. The LQI computes an optimal state-feedback control law for the tracking loop shown in the Fig. 7. For a plant (boost converter) with the state-space equations:

$$\begin{aligned} \frac{dx}{dt} &= Ax + Bu \\ y &= Cx + Du \end{aligned} \tag{17}$$

The state-feedback control is of the form:

$$u = -K[x, x_i] \tag{18}$$

where x_i is the integrator output and K is the optimal gain matrix. This control law ensures that the output V_{PV} tracks the reference command V_{ref} . The control law $u = -Kz = -K[x; x_i]$ minimizes the following cost functions (for $V_{ref} = 0$):

$$J(u) = \int_0^{\infty} \{z^T Qz + u^T Ru + 2z^T Nu\} dt \tag{19}$$

where Q , R and N are weighting matrices.

In (19), the energy of the states is penalized by matrix Q ; the matrix R penalizes the energy represented by the inputs; also the combinations of various inputs and states are penalized by matrix N .

All members of the matrix were originally chosen to have a value equal to the square of the reciprocal of the extreme value in each relevant variable. This means that all the variables are weighted with such a value that is proportional to the boundary that can be reached by the given parameter. After selecting the initial values, an initial simulation was implemented, whose results are utilized to adjust the parameters of the system to attain a controller which generates the essential time domain criteria such as rapid response time, low settling time and so on.

For the matrix Q , that is the weight matrix for the augmented state variables, the state deviations of the original model are mostly penalized with smaller weights, i.e. the change of these state variables is generally allowed. It is significantly different when one evaluates the last elements, which stand for the augmented states, i.e. the error terms. It can be stated, that those variables, which have a normal operating range are weighted with smaller weights, while those having a larger range have slightly larger weights. To realize acceptable tracking capabilities, the weight of the error term should be selected slightly high.

The matrix R is responsible for the weights of the inputs, i.e. how much the input parameters can be effective in the goal of the control.

With the examining of the impact of the third term in (19), it can be concluded that it penalizes the cross impacts of different states and input combinations. In this paper, the matrix N which has a size of 3x1 frequently comprises zeros. Regarding the matrix multiply operations in (19), the last

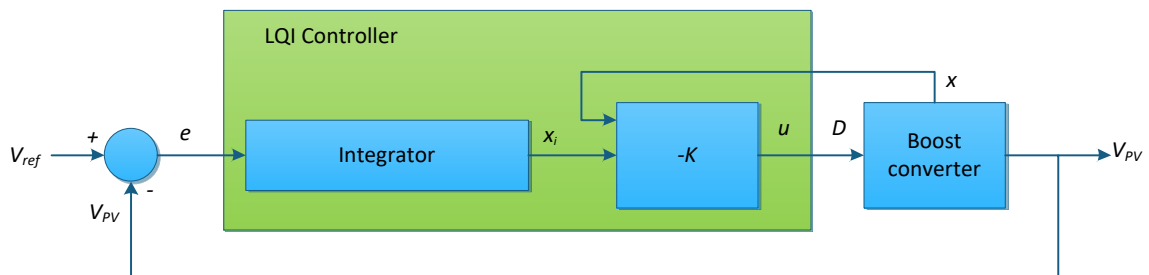


Fig. 7. Tracking loop based optimal state-feedback control law

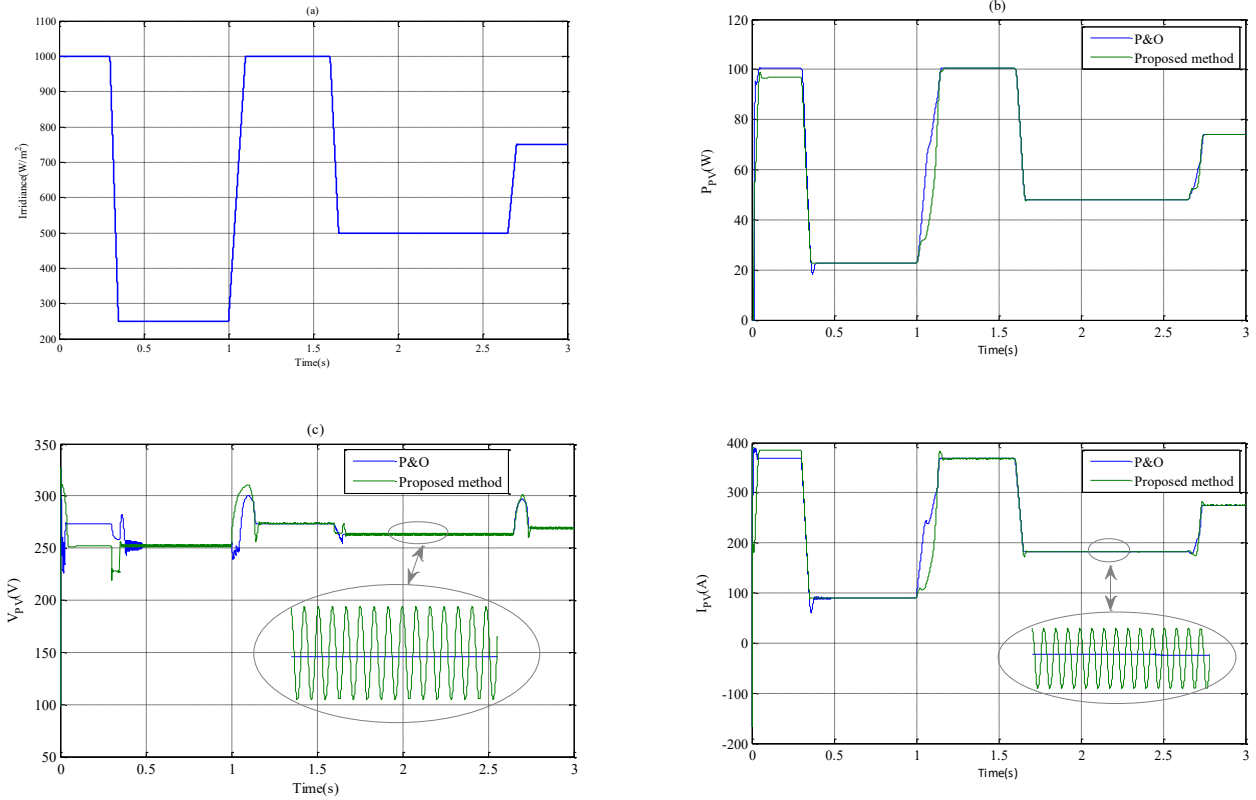


Fig. 8. Irradiation changes Test (a): The Irradiance variations (b): Active power of the PV system(c): Output voltage (d): Output current

element of matrix N represents the error term.

Next, the controllability of the augmented system should be checked. For this purpose, the extended system and input matrices including the feedback from the output can be represented by:

$$\hat{A} = \begin{bmatrix} A & 0 \\ -C & 0 \end{bmatrix}; \hat{B} = \begin{bmatrix} B \\ 0 \end{bmatrix} \quad (20)$$

The augmented system is controllable if and only if the controllability matrix defined by (21) has the same rank as the dimension of the state space representation.

$$Co = \begin{bmatrix} \hat{B} & \hat{A}\hat{B} & \hat{A}^2\hat{B} & \dots & \hat{A}^{n-1}\hat{B} \end{bmatrix} \quad (21)$$

The optimal gain matrix K can be obtained by:

$$K = R^{-1}\hat{B}^T P N \quad (22)$$

where matrix P can be obtained by solving the following control algebraic Riccati equation (CARE):

$$\hat{A}^T P + P \hat{A} - (P \hat{B} + N) R^{-1} (\hat{B}^T P + N^T) + Q = 0 \quad (23)$$

6.SIMULATION RESULT

This study utilizes MATLAB/SIMULINK to implement the proposed controller. We examine the performance of the

suggested GMPPT controller in the unshaded and shaded cases.

6.1. Irradiance changes

This test aims to check several probable linear irradiance trajectory changes shown in Fig. 8 (a). Besides, in Figs. 8 (b-d), the MPPT functioning of the suggested approach and the conventional P&O algorithm are displayed.

As displayed in Fig. 8(a), at $t=0.35s$, the trajectory reaches $S=250 \text{ W/m}^2$ form $S=1000 \text{ W/m}^2$. At $t=1.1s$, with increase step, the irradiance is equal to $S=1000 \text{ W/m}^2$. In the end, at $t=1.65s$ and $t=2.7s$, the irradiance levels decrease to $S=500 \text{ W/m}^2$ and increase to $S=750 \text{ W/m}^2$ respectively. By means of variations, dynamic and steady-state behaviors are analyzed.

In Figs. 8(c) and (d), the PV system voltage and current are drawn. The oscillatory behavior of the P&O algorithm in tracking the I_{MPP} is obviously visible. Instead, the proposed approach tracks the global MPP with minimum error. So, the active power tracks the reference values smoothly at all times.

6.2.Sinusoidal irradiance changes

The next test applies a sinusoidal irradiance plotted in Fig. 9 (a) to the PV-array. The test results are plotted in Figs. 9 (b). Clearly, the suggested approach forces the PV system to track the MPP with minimum error. Also, large amounts of error in P_{pv} , V_{pv} and I_{pv} are observable in the result of P&O algorithm. Once more, the superiority of the suggested GMPPT is verified due to little tracking error and minimal oscillations and consequently, very insignificant active power oscillations.

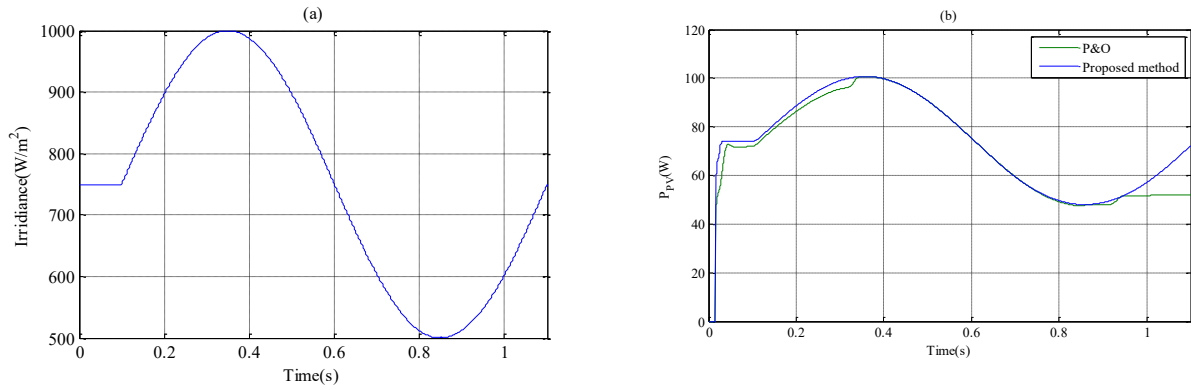


Fig. 9. Sinusoidal irradiance changes test; (a) The Irradiance variations, (b) Active power of the PV system

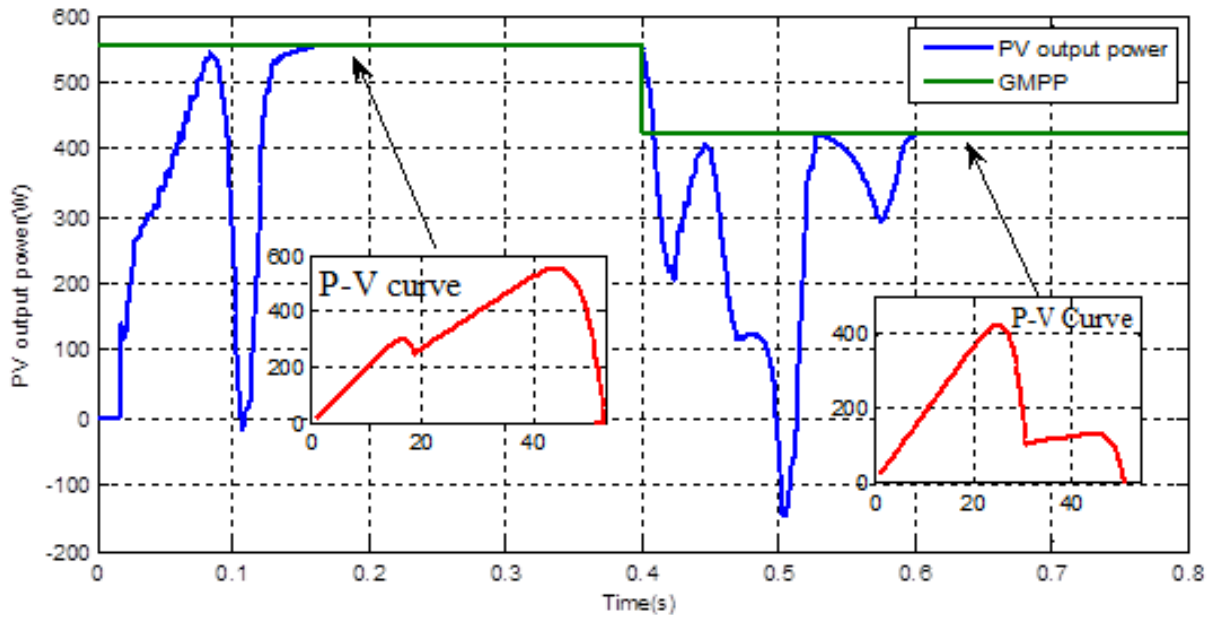


Fig. 10. Active power of the PV system under a partial shading condition test

6.3.A partial shading condition test

To show the effectiveness of the suggested MPPT controller in partial shading condition, we assume that one shaded PV module receives 600 W/m^2 another module receives 400 W/m^2 at $t=0\text{s}$ and they receive irradiance level of 100 and 550 W/m^2 at $t=0.4\text{s}$, respectively. According to the P-V characteristic curves drawn in Fig. 10, there are one global maximum power point and one local maximum power point. It is clear from this Figure that the proposed GMPPT converges to the GMPP with satisfactory accurate. It should be noted that from $t=0$ to $t=0.15\text{s}$, the proposed reference voltage estimator is searching the voltage corresponding to maximum power. As seen in the Fig. 10, from $t=0$ to $t=0.15\text{s}$, the two maximum power points at $t= 0.03\text{s}$ and $t= 0.84\text{s}$ are found by the proposed method. The reference voltage corresponding to the global maximum power point is at $t= 0.84\text{s}$. Although the global maximum point was found at $t=0.84\text{s}$, however, the algorithm presented in subsection 5.1 should be fully run to check the whole P-V curve shown in Fig. 10, because the point found at $t=0.84\text{s}$ may be one of the local points and global point is after this

point. The searching algorithm is completed at $t=0.12\text{s}$. After searching the whole curve, the reference voltage corresponding to the global maximum power point is applied to the LQI to deliver the maximum power to the load. In similar, when the irradiance level is varied, the reference voltage estimator search the voltage corresponding to the maximum power.

6.4.A comparative study for a normal condition

This subsection presents a comparative study between the proposed approach and method proposed in [42]. This reference proposes an Improved Double Integral Sliding Mode MPPT Controller (IDISMC) as an MPPT method for a photovoltaic system. The results of the comparison are shown in Figs. 11. As seen in these Figures, the proposed approach makes a better control effort for the MPPT. Moreover, for the period of the ramp, the IDISMC causes the PV power to oscillate around the MPP.

6.5.A comparative study for a partial shading condition

Fig. 12 shows a comparative study in a partial shading

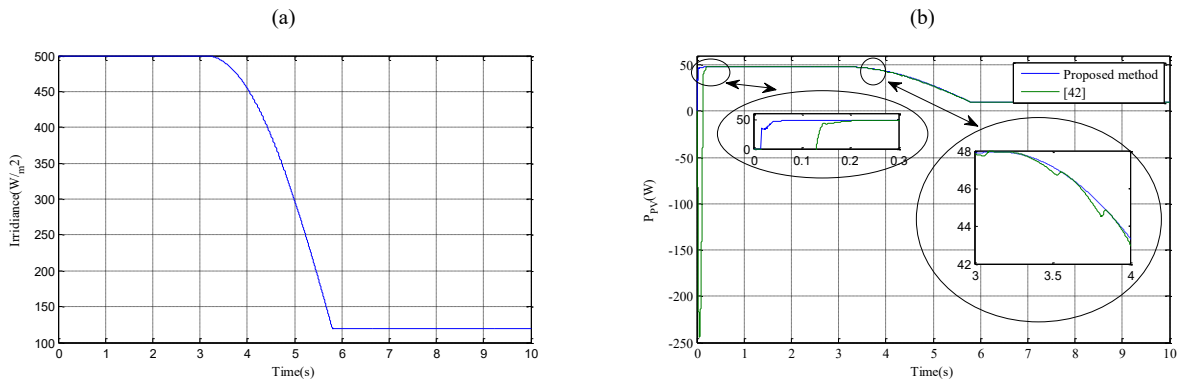


Fig. 11. The results of comparative study for the unshaded condition; (a) irradiation variations, (b) Active power of the PV system

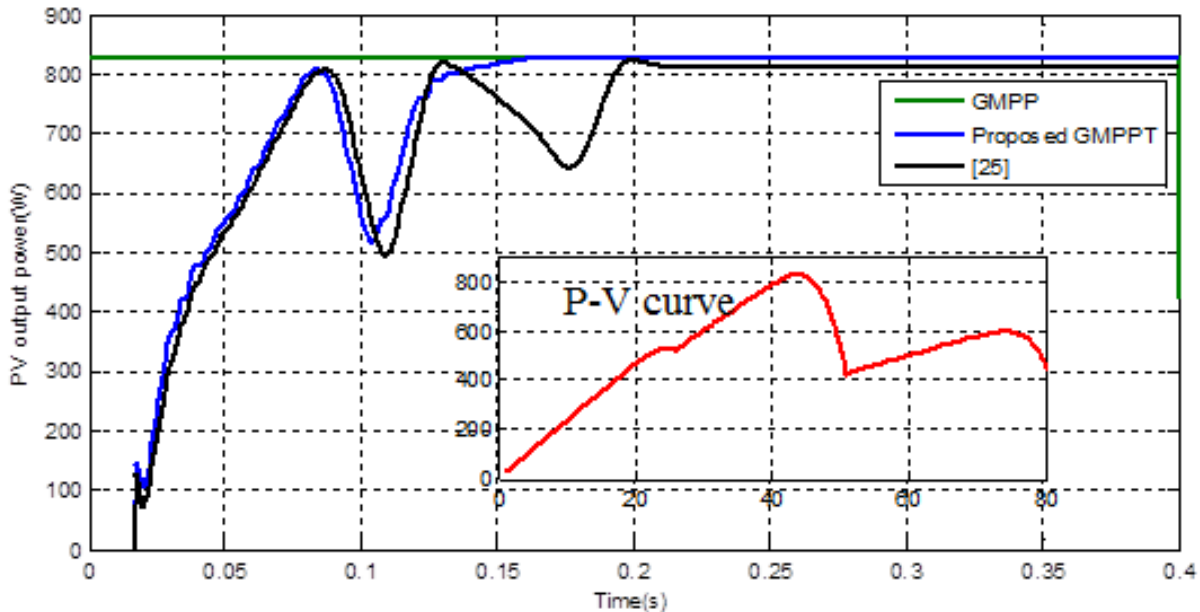


Fig. 12. The results of comparative for the partial shading condition; (a) Active power of the PV system, (b) P-V curve under the partial shading condition

condition between the suggested GMPPT and method proposed in [25]. According to the P-V characteristic curve drawn in Fig. 12, the amount of the GMPP is 829.9 W. As seen in Fig. 12, all methods converge to the GMPP, however, the proposed GMPPT has converged to the GMPP with the quickest response and the smallest error (less than 1 watt).

It should be noted that from $t=0$ to $t=0.17s$, the three maximum power points at $t=0.03s$, $t=0.81s$, $t=0.98s$ are found by the proposed method. The reference voltage corresponding to the global maximum power point is at $t=0.81s$.

1.CONCLUSION

In PV systems, MPPT algorithms are utilized to transfer the maximum power to the load and as a result of enhancing the efficiency. Important issues in designing the MPPT methods contain the complexity of the system, dynamical performance, and uncertainty. This study introduces new two-level control architecture to perform the GMPPT tasks. A new algorithm is proposed to estimate the reference voltage in the unshaded and shaded conditions. A LQI controller uses

the estimated reference voltage to generate the optimal duty cycle for a boost converter to transfer the maximum power point from PV systems to load. The results confirm that the PV system using the suggested GMPPT Tracker converges to the GMPP in the unshaded and shaded conditions. The method proposed in this paper can be easily implemented in an experiment work and there is no specific limitation to implement the proposed method in a realistic work.

APPENDIXES

Appendix 1: Boost converter parameters

- Output capacitance (C)= 330 μ F
- Load resistance (R_L) =50 Ω
- Nominal duty ratio (D) =0.8
- Inductance(L) =120 μ H

Appendix 2: LQI Parameters

- Q=[10.5 0.33
- 0.50 1 0.67
- 0.33 0.67 10],

$$R=0.1,$$

$$N=[0 \ 0 \ 10]^T,$$

$$K= [133.98 \quad 42471.270.22];$$

REFERENCES

- [1] ESRAM T, CHAPMAN PL. Comparison of photovoltaic array maximum power point tracking techniques. *IEEE Trans Energy Convers* 2007;22(2):439–49.
- [2] De Brito MAG, Galotto L, Sampaio LP, de Azevedo e Melo G, Canesin CA. Evaluation of the main MPPT techniques for photovoltaic applications. *IEEE Trans Indus Electr* 2013;60(3):1156–67.
- [3] Ishaquea K, Salamb Z. A review of maximum power point tracking techniques of PV system for uniform insolation and partial shading condition. *Renew Sustain Energy Rev* 2013;19(March):475–88.
- [4] Jain S, Agarwal V. Comparison of the performance of maximum power point tracking schemes applied to single-stage grid-connected photovoltaic systems. *IET Electr Power Appl* 2007;1(5):753–62.
- [5] Femia N, Granozio D, Petrone S, Spagnuolo G, Vitelli M. Predictive & adaptive MPPT perturb and observe method. *IEEE Trans Aerosp Electron Syst* 2007;43(3):934–50.
- [6] Casadei D, Grandi G, Rossi C. Single-phase single-stage photovoltaic generation system based on a ripple correlation control maximum power point tracking. *IEEE Trans Energy Convers* 2006;21(2):562–8.
- [7] Abdelsalam AK, Massoud AM, Ahmed S, Enjeti P. High-performance adaptive perturb and observe MPPT technique for photovoltaic-based microgrids. *IEEE Trans Power Electron* 2011;26(4):1010–21.
- [8] Qiang M, Mingwei S, Liying L, Guerrero JM. A novel improved variable step-size incremental-resistance MPPT method for PV systems. *IEEE Trans Industr Electron* 2011;58(6):2427–34.
- [9] Fangrui L, Shanxu D, Fei L, Bangyin L, Yong K. A variable step size INC MPPT method for PV systems. *IEEE Trans Industr Electron* 2008;55(7):2622–8.
- [10] Sera D, Teodorescu R, Hantschel J, Knoll M. Optimized maximum power point tracker for fast-changing environmental conditions. *IEEE Trans Industr Electron* 2008;55(7):2629–37.
- [11] Weidong X, Ozog N, Dunford WG. Topology study of photovoltaic interface for maximum power point tracking. *IEEE Trans Industr Electron* 2007;54(3):1696–704.
- [12] Karlisa AD, Kottasb TL, Boutalibb YS. A novel maximum power point tracking method for PV systems using fuzzy cognitive networks (FCN). *Electric Power Syst Res* 2007;77(3–4):315–27.
- [13] Kulaksız AA, Akkaya R. A genetic algorithm optimized ANN-based MPPT algorithm for a stand-alone PV system with induction motor drive. *Sol Energy* 2012;86(9):2366–75.
- [14] Bahgata ABG, Helwab NH, Ahmadb GE, El Shenawyb ET. Maximum power point tracking controller for PV systems using neural networks. *Renew Energy* 2005;30(8):1257–68.
- [15] Hiyama, Takashi, and Ken Kitabayashi. "Neural network based estimation of maximum power generation from PV module using environmental information." *IEEE Transactions on Energy Conversion* 12.3 (1997): 241-247.
- [16] Salah CB, Ouali M. Comparison of fuzzy logic and neural network in maximum power point tracker for PV systems. *Electric Power Syst Res*. 2011;81(1):43–50.
- [17] Elobaid LM, Abdelsalam AK, Zakzouk EE. Artificial neural network based maximum power point tracking technique for PV systems. In: *Proc of 38th annual conference on IEEE industrial electronics society, IECON*; 2012. p. 937–42.
- [18] Chiu YH, Luo YE, Huang JW, Liu YH. An ANN-based maximum power point tracking method for fast changing environments. In: *Proc of 13th international symposium on advanced intelligent systems*; 2012. p. 715–20.
- [19] Seo JH, Im CH, Heo CG, Kim JK, Jung HK, Lee CG. Multimodal function optimization based on particle swarm optimization. *IEEE Trans Magn* 2006;42(4):1095–8. <http://dx.doi.org/10.1109/TMAG.2006.871568>.
- [20] Miyatake M, Veerachary M, Toriumi F, Fujii N, Ko H. Maximum power point tracking of multiple photovoltaic arrays: a PSO approach. *IEEE Trans Aerosp Electron Syst* 2011;47(1):367–80.
- [21] Koutroulis E, Blaabjerg F. A new technique for tracking the global maximum power point of PV arrays operating under partial-shading conditions. *IEEE J Photovoltaics* 2012;2(2):184–90.
- [22] Nguyen TL, Low K-S. A global maximum power point tracking scheme employing DIRECT search algorithm for photovoltaic systems. *IEEE Trans Industr Electron* October 2010;57(10):3456–67.
- [23] Ji YH, Jun DY, Kim JG, Kim JH, Lee TW, Won CY. A real maximum power point tracking method for mismatching compensation in PV array under partially shaded conditions. *IEEE Trans Power Electron* 2011;26(4):1001–9.
- [24] Patel H, Agarwal V. Maximum power point tracking scheme for PV systems operating under partially shaded conditions. *IEEE Trans Ind Electron* 2008;55(4):1689–98.
- [25] Boztepe M, Guinjoan F, Velasco-Quesada G, Silvestre S, Chouder A, Karatepe E. Global MPPT scheme for photovoltaic string inverters based on restricted voltage window search algorithm. *IEEE Trans Industr Electron* 2014;61(7):3302–12.
- [26] Syafaruddin, Karatepe E, Hiyama T. Artificial neural network-polar coordinated fuzzy controller based maximum power point tracking control under partially shaded conditions. *IET Renew Power Gener* 2009;3(2):239–53.
- [27] Alajmi BN, Ahmed KH, Finney SJ, Williams BW. A maximum power point tracking technique for partially shaded photovoltaic systems in microgrids. *IEEE Trans Industr Electron* 2013;60(4):1596–606.
- [28] Peng L, Yaoyu L, Seem JE. Sequential ESC-based global MPPT control for photovoltaic array with variable shading. *IEEE Trans Sustain Energy* 2011;2(3):348–58.
- [29] Kazmi S, Goto H, Ichinokura O, Guo Hai-Jiao. An improved and very efficient MPPT controller for PV systems subjected to rapidly varying atmospheric conditions and partial shading. In: *Proc of the Australasian power engineering conference*; 2009. p. 1–6.
- [30] Ahmed J, Salam Z. A maximum power point tracking (MPPT) for PV system using Cuckoo Search with partial shading capability. *Appl Energy* 2014;119(15):118–30.
- [31] Mamarelis E, Petrone G, Spagnuolo G. A two-steps algorithm improving the P&O steady state MPPT efficiency. *Appl Energy* 2014;113(January):414–21.
- [32] Punitha K, Devaraj D, Sakthivel S. Artificial neural network based modified incremental conductance algorithm for maximum power point tracking in photovoltaic system under partial shading conditions. *Energy* 2013;62(1):330–40.
- [33] Ishaque K, Salam Z, Shamsudin A, Amjad M. A direct control based maximum power point tracking method for photovoltaic system under partial shading conditions using particle swarm optimization algorithm. *Appl Energy* 2012;99(April):414–22.
- [34] Ghosh A, Dehuri S. Evolutionary algorithms for multi-criterion optimization: a survey. *Int J Comput Inform Sci* 2004;2(1):38–57.
- [35] Daraban S, Petreus D, Morel C. A novel global MPPT based on genetic algorithms for photovoltaic systems under the influence of partial shading. In: *39th annual conference of the IEEE industrial electronics society, IECON*; 2013.
- [36] Sareni B, Krahenbuhl L. Fitness sharing and niching method revisited. *IEEE Trans Evol Comput* 1998;2(3):97–106. <http://dx.doi.org/10.1109/4235.735432>.
- [37] Hooke R, Jeeves TA. Direct search solution of numerical and statistical problems. *J Assoc Comput Mach* 1961;8(2):212–29.
- [38] Dilettoso E, Rizzo SA, Salerno N. A parallel version of the self-adaptive low high evaluation evolutionary-algorithm for electromagnetic device optimization. *IEEE Trans Magn* 2014;50(2):633–6. <http://dx.doi.org/10.1109/TMAG.2013.2284928>.
- [39] Liu YH, Chen JH, Huang JW. Global maximum power point tracking algorithm for PV systems operating under partially shaded conditions using the segmentation search method. *Sol Energy* 2014;103(May):350–63.
- [40] N. Femia, G. Petrone, G. Spagnuolo, and M. Vitelli, *Power Electronics and Control Techniques for Maximum Energy Harvesting in Photovoltaic Systems* (CRC Press, 2012).
- [41] C. S. Solanki, *Solar Photovoltaics: Fundamentals, Technologies and*

Applications (PHI Learning Pvt. Ltd., 2015).

- [42] Chatrenour, N., Razmi, H., & Doagou-Mojarrad, H. Improved double integral sliding mode MPPT controller based parameter estimation for a stand-alone photovoltaic system. *Energy Conversion and Management* 2017, 139, 97-109.
- [43] Habibi, Mehran, and Alireza Yazdizadeh. "New MPPT controller

design for PV arrays using neural networks (Zanjan City Case Study)." *International Symposium on Neural Networks*. Springer, Berlin, Heidelberg, 2009.

- [44] F. Blaabjerg, Z. Chen, and S. B. Kjaer, "Power electronics as efficient interface in dispersed power generation systems," *IEEE Trans. Power Electron.* 19(5), 1184–1194 (2004).

HOW TO CITE THIS ARTICLE

M. Rahideh, A. Halvaei Niasar, A. Ketabi, I. Zamani, Linear Quadratic Integral optimal control of photovoltaic systems, AUT J. Elec. Eng., 52(2) (2020) 231-242.

DOI: [10.22060/ej.2020.14970.5249](https://doi.org/10.22060/ej.2020.14970.5249)



